

Recent Developments in Neutrino-Nucleus Scattering (Theory)

Satoshi X. Nakamura

Department of Physics, Osaka University, Toyonaka, Osaka 560-0043, Japan

Selected theoretical developments in neutrino-nucleus scattering in 2015-2016 are reviewed.

1 Introduction

Next-generation neutrino oscillation experiments are going to address the leptonic CP violation and the neutrino mass hierarchy, and for this purpose, more accurate understanding of neutrino-nucleus reactions is needed. Because the neutrino oscillation experiments utilize neutrino beams over a wide energy range, the neutrino-nucleus reactions of different characteristics need to be understood. From low to high energies, the dominant reaction mechanism varies from the quasi-elastic knockout of a nucleon (QE), quasi-free excitation of the $\Delta(1232)$ or higher resonances followed by a decay into a meson-baryon final state (RES), and deep inelastic scattering (DIS). A unified description of the neutrino-nucleus reactions over the wide energy range needs to be developed; recent efforts towards this direction are reported in Ref.¹. In this review presentation, I will cover selected theoretical developments in 2015-2016 in neutrino-nucleus scattering in the QE and RES regions.

2 QE

The neutrino-nucleus scattering in the QE region is highly relevant to the T2K experiment² that utilizes relatively low-energy neutrino beam peaking at ~ 0.6 GeV. Recent theoretical interest in this subject has been to better understand QE-like processes such as those involving meson-exchange currents and final state interactions (FSI)³. Here I will focus on a very recent update on the subject: an ab initio calculation of inclusive electron scattering on ^{12}C in the QE region^{4,5}. Ab initio calculations are presumably the best approach in non-relativistic regime, apart from rather expensive computational cost. Although this work is about the electron scattering, the same method should work as well for neutrino scattering. Also, the approach can be validated against a large amount of precise electron scattering data.

In the ab initio approach to nuclear many-body problems, one exactly (up to a certain numerical accuracy) solves the Schrödinger equation, $H|\Psi_i\rangle = E_i|\Psi_i\rangle$, where E_i is an energy eigenvalue and $|\Psi_i\rangle$ is the corresponding eigen-vector. The nuclear Hamiltonian is given by $H = \sum_i p_i^2/2m_N + \sum_{i<j} v_{ij} + \sum_{i<j<k} v_{ijk} + \dots$, where the first, second, and third terms are the kinetic term, NN potential, and $3N$ potential, respectively. This nuclear many-body problem has been solved with the Green's function Monte Carlo (GFMC) method, which is one of ab initio calculational methods, and the result excellently reproduced data for ground and low-lying excited state energies of light nuclei up to and including $A = 12$ (A : mass number)⁶. This state-of-the-art technology has been applied to the inclusive electron scattering^{4,5}.

The electron scattering is induced by electromagnetic current operators acting on a nuclear wave function. The currents used in Refs. ^{4,5} consist of one-body impulse current and two-body meson-exchange currents. The currents are constrained by the current conservation, and also by data such as magnetic moments and electromagnetic form factors of light nuclei. With the transverse (longitudinal) electromagnetic current operators, J_T (J_L), the corresponding response function is defined by

$$R_\alpha(\omega, \vec{q}) = \sum_f \langle \Psi_0 | J_\alpha^\dagger(\omega, \vec{q}) | \Psi_f \rangle \langle \Psi_f | J_\alpha(\omega, \vec{q}) | \Psi_0 \rangle \delta(\omega + E_0 - E_f), \quad \alpha = L, T \quad (1)$$

where ω (\vec{q}) denotes the energy (momentum) transfer from the electron to the nucleus; Ψ_0 (Ψ_f) is the ground (an excited) state with the corresponding energy E_0 (E_f). The cross sections for the inclusive electron scattering on the nucleus can be expressed with the response functions that encode information of the nuclear dynamics.

The authors of Refs. ^{4,5} calculated the response functions for ^{12}C . Because a direct evaluation of the response functions is formidably difficult, they took a strategy to first evaluate the Laplace transform of $R_\alpha(\omega, \vec{q})$ with the GFMC method, and then invert it to obtain $R_\alpha(\omega, \vec{q})$; for the inversion, the maximum entropy method was employed. The obtained transverse response, $R_T(\omega, \vec{q})$, divided by the square of $G_E^p(\omega, \vec{q})$ (the electric form factor of the proton) is shown in Fig. 1 where experimental data are also shown for a comparison. The calculation done with both one- and two-body currents (only one-body current) is labelled by 'GFMC O_{1b+2b} ' ('GFMC O_{1b} ') in the figure. It is clearly seen in the figure that the response functions of GFMC O_{1b+2b} agree with the data excellently, and are significantly enhanced from those of GFMC O_{1b} over the whole ω region. Also shown in Fig. 1 is 'PWIA' which is the plane-wave impulse approximation and is calculated with the single nucleon momentum distribution of ^{12}C from Ref. ⁹. The response functions of GFMC O_{1b} and those of PWIA are significantly different, indicating a large reduction due to FSI. These results validate the predictive power of the ab initio approach in this kinematical regime. Other nuclear many-body models that involve approximations and/or truncations of model space should be validated by either data or the ab initio calculations.

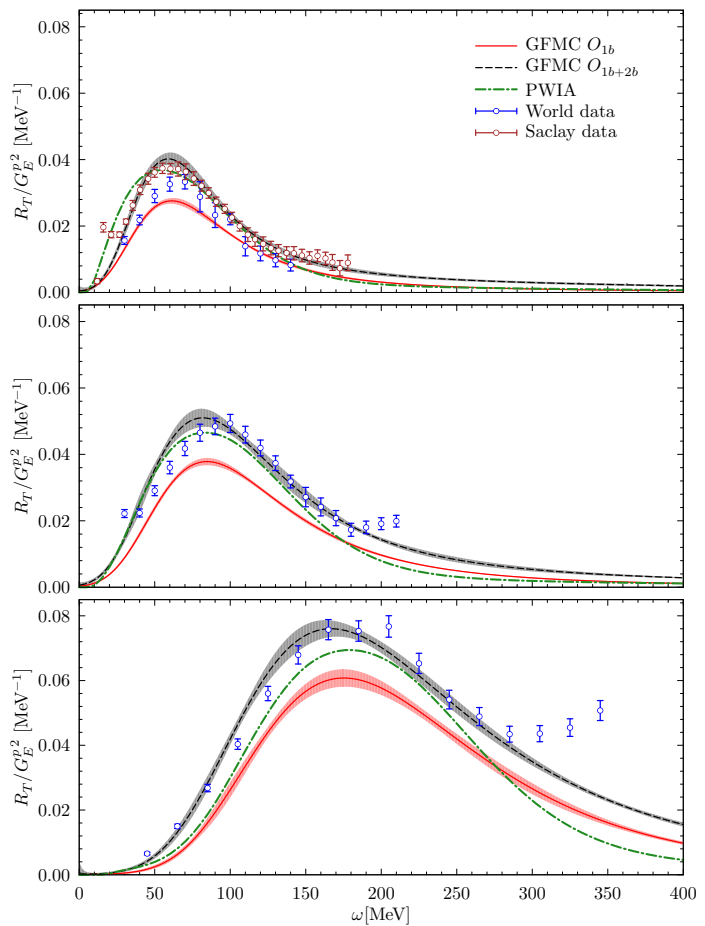


Figure 1 – (Color online) Transverse response functions for inclusive electron scattering on ^{12}C . The top, middle, and bottom figures are for $|\vec{q}| = 300, 380,$ and 570 MeV, respectively. Data are from the world data analysis⁷ and from Saclay⁸. Figures taken from Ref.⁵. Copyright (2016) APS.

3 RES

The neutrino-nucleus scattering in the RES region is relevant to low-energy ($E_\nu \lesssim 1$ GeV) experiments such as T2K² where a pion produced by $\Delta(1232)$ can be stuck in the nucleus, giving a CCQE-like event. It is also relevant to relatively high-energy ($E_\nu = 2 \sim 4$ GeV) experiments such as DUNE¹⁰ where higher resonances are excited to produce one or two pions. For theoretically describing the processes, we need nuclear models that describe initial nucleon correlations, FSI, and medium modifications of hadron properties. We also need a model that describes neutrino reactions on a single nucleon. Elementary amplitudes from the model are a building block to construct a neutrino-nucleus scattering model. In what follows, I will focus on two recent works for developing an elementary process model in the RES region.

3.1 Dynamical coupled-channels model for neutrino-induced meson productions

In the RES region, particularly between the $\Delta(1232)$ and DIS regions, developing a model for neutrino-induced meson productions off a single nucleon is still an issue. Several theoretical models have been developed, and particularly the $\Delta(1232)$ region has been extensively studied because of its importance. However, there still remain conceptual and/or practical problems in the existing models as follows: First, reactions in the RES region are multi-channel processes in nature. However, no existing model takes account of the multi-channel couplings required by the unitarity. Second, neutrino-induced double pion productions over the entire RES region have not been studied in detail previously, even though their production rates are expected to be comparable or even more important than those for the single-pion productions around and beyond the second RES region. Third, interference between resonant and non-resonant amplitudes are not well under control for the axial current in most of the previous models. In Ref.¹¹, the authors developed a neutrino-nucleon reaction model in the RES region by overcoming the problems mentioned above; this is what I will review in this subsection.

For developing a neutrino-nucleon reaction model in the RES region, the authors of Ref.¹¹ took the best available option: working with a coupled-channels model. In the last few years, the authors' group have developed a dynamical coupled-channels (DCC) model to analyze $\pi N, \gamma p \rightarrow \pi N, \eta N, K\Lambda, K\Sigma$ reaction data for a study of the baryon spectroscopy¹². In there, they have shown that the model is successful in giving a reasonable fit to a large amount ($\sim 23,000$ data points) of the data in the RES region. The model also has been shown to give a reasonable prediction for pion-induced double pion productions¹³. Thus the DCC model seems a promising starting point for developing a neutrino-reaction model in the RES region. For extending the DCC model to the sector of neutrino reactions, the authors of Ref.¹¹ made the following developments. Regarding the vector current, they already had fixed the amplitude for the proton target at $Q^2=0$ in their previous analysis¹². The remaining task was to determine the Q^2 -dependence of the vector couplings, i.e., form factors. This was achieved by analyzing data for the single pion electroproduction and inclusive electron scattering. A similar analysis was also done for the neutron target data. By combining the vector current amplitudes for the proton and neutron targets, the isospin separation of the vector current amplitudes was made; this is a necessary step for applying the vector current amplitudes to the neutrino reactions. Regarding the axial current, its matrix elements for tree-level non-resonant processes were derived from the chiral Lagrangian; the same Lagrangian has been used to derive the $\pi N \rightarrow MB$ (MB : a meson-baryon state) potentials in the DCC model. By construction, the PCAC relation is satisfied. Because of rather scarce neutrino reaction data, it is difficult to determine $N-N^*$ transition matrix elements induced by the axial current. The conventional practice is to write down a $N-N^*$ transition matrix element induced by the axial current in a general form with three or four form factors. Then the PCAC relation is invoked to relate the presumably most important axial form factor to the corresponding πNN^* coupling. The other form factors are ignored except for the pion pole term. In Ref.¹¹, the axial currents for bare N^* of the spin-parity

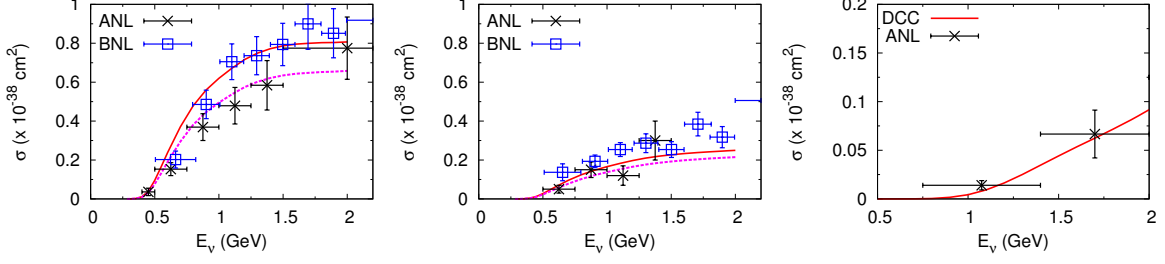


Figure 2 – (Color online) Comparison of the DCC-based calculation (red solid curves) with data for $\nu_\mu p \rightarrow \mu^- \pi^+ p$ (left), $\nu_\mu n \rightarrow \mu^- \pi^0 p$ (middle) and $\nu_\mu p \rightarrow \mu^- \pi^+ \pi^0 p$ (right). The DCC calculation with $0.8 \times g_{AN\Delta(1232)}^{PCAC}$ is also shown (magenta dashed curve). The data are from ANL¹⁴ and BNL¹⁵ in the left and middle panels, and ANL data are from Ref.¹⁶ in the right panel. Figures taken from Ref.¹¹. Copyright (2015) APS.

$1/2^\pm$, $3/2^\pm$, $5/2^\pm$ and $7/2^\pm$ were considered, and the above procedure was taken to determine their axial form factors at $Q^2 = 0$. As a result of this derivation, the interference pattern between the resonant and non-resonant amplitudes are uniquely fixed within their DCC model; this is a great advantage of the DCC approach. For the Q^2 -dependence of the axial-current matrix elements, a simple ansatz was taken inevitably due to the lack of experimental information. This is a limitation shared by all the existing neutrino-reaction models in the RES region. The Q^2 -dependence of all the axial-coupling was assumed to be the conventional dipole form with the axial mass, $M_A = 1.02$ GeV.

With the vector and axial currents as described above, cross sections for the neutrino-induced meson productions in the RES region were calculated. The calculated CC neutrino-induced single pion production cross sections from the DCC model are compared with available data from Refs.^{14,15} in Fig. 2 (left, middle). The left panel shows the total cross sections for $\nu_\mu p \rightarrow \mu^- \pi^+ p$ for which $\Delta(1232)$ dominates. The two datasets from ANL¹⁴ and BNL¹⁵ for $\nu_\mu p \rightarrow \mu^- \pi^+ p$ shown in the left panel of Fig. 2 are not consistent as has been well known, and the DCC calculation is closer to the BNL data¹⁵. For the neutron target (middle), the DCC calculation is fairly consistent with both of the ANL and BNL data. It seems that the bare axial N - $\Delta(1232)$ coupling constants determined by the PCAC relation are too large to reproduce the ANL data. Thus the bare axial N - $\Delta(1232)$ coupling constants, $g_{AN\Delta(1232)}^{PCAC}$, is multiplied by 0.8 so that the DCC model better fits the ANL data. The resulting cross sections are shown by the dashed curves in Fig. 2 (left,middle). We see that $\sigma(\nu_\mu p \rightarrow \mu^- \pi^+ p)$ is reduced due to the dominance of the $\Delta(1232)$ resonance in this channel, while $\sigma(\nu_\mu n \rightarrow \mu^- \pi N)$ is only slightly reduced. The original data of these two experimental data have been reanalyzed recently¹⁷, and it was claimed that the discrepancy between the two datasets is resolved. The resulting cross sections are closer to the original ANL data. It is noted that the data shown in Fig. 2 were taken from experiments using the deuterium target. Thus one should analyze the data considering the nuclear effects such as the initial two-nucleon correlation and the final state interactions. In the next subsection, I review a recent work¹⁸ that took a first step toward such an analysis.

Next the DCC calculation for a double-pion production is compared with existing data in Fig. 2 (right). Although there exist a few theoretical works on the neutrino-induced double-pion production near threshold, this DCC calculation is the first one that took account of relevant resonance contributions for this process. The DCC-based prediction is in good agreement with the data for the $\nu_\mu p \rightarrow \mu^- \pi^+ \pi^0 p$ cross sections. For a fuller presentation of the DCC calculations, see Ref.¹¹.

3.2 Effects of final state interactions on pion productions in neutrino-deuteron reactions

The bubble chamber experiments at ANL¹⁴ and BNL¹⁵ measured cross sections for $\nu_\mu d \rightarrow \mu^- \pi NN$ (d : deuteron) and, from the data, the elementary $\nu_\mu N \rightarrow \mu^- \pi N$ cross sections were

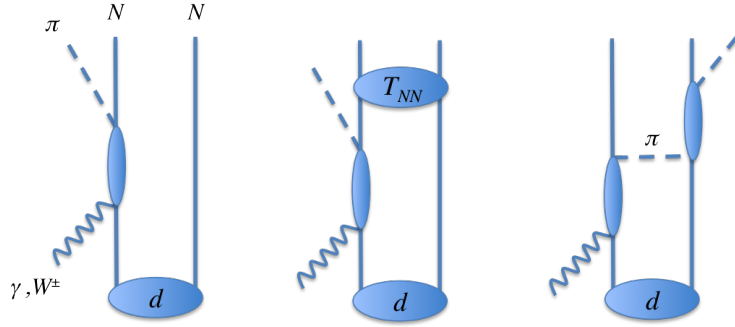


Figure 3 – Mechanisms considered in Ref.¹⁸ for describing $\gamma d (W^\pm d) \rightarrow \pi NN$ reactions. (Left) Impulse term; (Middle) NN rescattering term; (Right) πN rescattering term.

extracted. However, the FSI was not taken into account in extracting the single nucleon cross sections. This is disturbing because the data (cross sections for the elementary processes)^{14,15} are essentially only available information to determine the strength of the dominant nucleon- $\Delta(1232)$ transition induced by the axial-current. Thus the uncertainty of the data^{14,15} is directly reflected in uncertainty of theoretical calculations for neutrino-nucleus cross sections. In this subsection, I review a recent work¹⁸ that studied the FSI effect on the $\nu_\mu d \rightarrow \mu^- \pi NN$ reactions.

The authors of Ref.¹⁸ used a dynamical model (called SL model) developed in Ref.¹⁹ to generate elementary amplitudes that go into a model for the neutrino-deuteron reactions. The SL model has been shown to reproduce well the electromagnetic pion production data in the $\Delta(1232)$ region, as well as the ANL and BNL data for the neutrino-induced single pion production cross sections. The incoherent electroweak pion productions on the deuteron were described in Ref.¹⁸ with the impulse term (Fig. 3 (left)), the NN rescattering term (Fig. 3 (middle)), and the πN rescattering term (Fig. 3 (right)). In the diagrams of Fig. 3, the $\gamma N (W^\pm N) \rightarrow \pi N$ and $\pi N \rightarrow \pi N$ amplitudes are generated by the SL model, while the NN scattering amplitudes and the deuteron wave function are obtained with the Bonn potential²⁰.

With the model described above, the authors of Ref.¹⁸ first studied pion photoproduction on the deuteron. Because there are precise and abundant data available for the process, they can confront the model with the data to examine the soundness of the model. Also, they can test the vector current with the photo-reaction data before using it for neutrino processes. Their calculation for $\gamma d \rightarrow \pi^0 pn$ total cross section is shown in Fig. 4. The figure illustrates how the FSI modify the cross sections calculated with the impulse term only. It is clearly seen that the NN rescattering effect largely reduces the cross sections, and brings the calculation much closer to the data. This large reduction can be understood as a consequence of the orthogonality between the deuteron and the pn scattering wave functions. On the other hand, the πN rescattering effect turned out to be rather small. The authors of Ref.¹⁸ also found that the FSI effect is small for the $\gamma d \rightarrow \pi^- pp$ cross section where the orthogonality does not work.

Having seen the capability of the model in the electromagnetic sector above, the model was then applied to the neutrino-induced pion productions. They chose a set of kinematical region where the cross section gets large, i.e., the quasi-free $\Delta(1232)$ -excitation kinematics. Thus, for $E_\nu = 1$ GeV, the muon kinematics is chosen to be $\theta_\mu = 25^\circ$ and $E_\mu = 550, 600, 650$ MeV. The result for the differential cross section for $\nu_\mu d \rightarrow \mu^- \pi^+ pn$ is shown in Fig. 5 as a function of the pion emission angle. The NN rescattering effect is again seen to be sizable. This is because the orthogonality between the deuteron and scattering pn state is at work. The πN rescattering effect is again rather small. In this way, Ref.¹⁸ showed that the FSI effect is quite sizable in the neutrino-induced pion production on the deuteron, although it had been ignored in the previous analyses^{14,15} for extracting cross sections of the elementary processes. The analysis of Ref.¹⁸ was limited to a certain kinematics as seen above, and thus they did not analyze the bubble chamber data^{14,15} to extract cross sections of the elementary processes. The data analysis requires

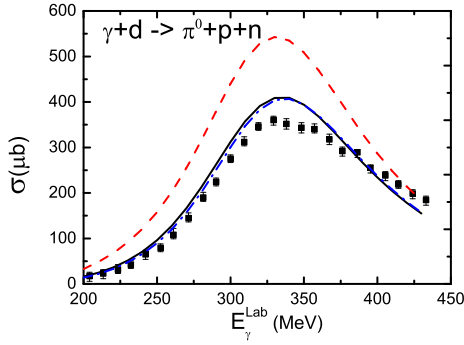


Figure 4 – (Color online) FSI effect on total cross sections for $\gamma d \rightarrow \pi^0 pn$ reaction. The red dashed curve is obtained with the impulse term only. By including the NN (NN and πN) rescattering terms, the blue dash-dotted (the black solid) curve is obtained. Figures taken from Ref.¹⁸. Copyright (2015) APS.

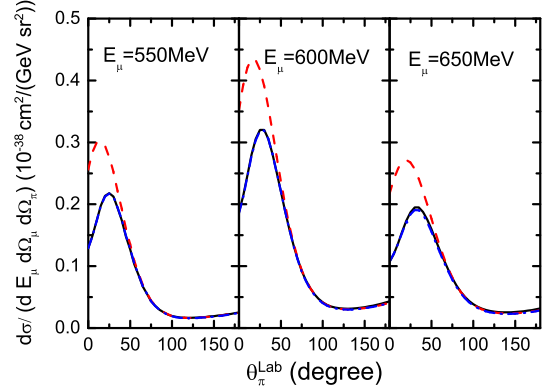


Figure 5 – (Color online) FSI effect on differential cross sections for $\nu_\mu d \rightarrow \mu^- \pi^+ pn$ reaction at $E_\nu = 1$ GeV, $\theta_\mu = 25^\circ$, $\phi_\pi = 0^\circ$. The features of the curves are the same as those in Fig. 4. Figures taken from Ref.¹⁸. Copyright (2015) APS.

integration all over the phase space, which is rather demanding computationally. Even so, considering that accurate cross section data for the elementary processes are highly demanded, it would be important to reanalyze the bubble chamber data with the sizable FSI effect taken into account.

Acknowledgments

My participation to NUFAC 2016 was supported by JSPS KAKENHI Grant Number JP25105010.

References

1. S.X. Nakamura et al.: arXiv:1610.01464
2. K. Abe et al. (T2K Collaboration): Nucl. Instrum. Meth. **A659** (2011) 106
3. L. Alvarez-Ruso, Y. Hayato, and J. Nieves: New J. Phys. **16** (2014) 075015
4. A. Lovato et al.: Phys. Rev. C **91** (2015) 062501
5. A. Lovato et al.: Phys. Rev. Lett. **117** (2016) 082501
6. J. Carlson et al.: Rev. Mod. Phys. **87** (2015) 1067
7. J. Jourdan: Nucl. Phys. **A603** (1996) 117
8. P. Barreau et al.: Nucl. Phys. **A402** (1983) 515
9. R.B. Wiringa, R. Schiavilla, S.C. Pieper, and J. Carlson: Phys. Rev. C **89** (2014) 024305
10. R. Acciarri et al. (DUNE Collaboration): arXiv:1512.06148
11. S.X. Nakamura, H. Kamano, T.-S. H. Lee, and T. Sato: Phys. Rev. D **92** (2015) 074024
12. H. Kamano, S.X. Nakamura, T.-S. H. Lee, and T. Sato: Phys. Rev. C **88** (2013) 035209
13. H. Kamano: Phys. Rev. C **88** (2013) 045203
14. S.J. Barish et al.: Phys. Rev. D **19** (1979) 2521
15. T. Kitagaki et al.: Phys. Rev. D **34** (1986) 2554
16. D. Day et al.: Phys. Rev. D **28** (1983) 2714
17. C. Wilkinson et al.: Phys. Rev. D **90** (2014) 112017
18. J.-J. Wu, T. Sato, and T.-S. H. Lee: Phys. Rev. C **91** (2015) 035203
19. T. Sato and T.-S. H. Lee: Phys. Rev. C **54** (1996) 2660;
T. Sato, D. Uno and T.-S. H. Lee: Phys. Rev. C **67** 065201 (2003)
20. R. Machleidt, in Advances in Nuclear Physics, edited by J.W. Negele and E. Vogt (Plenum, New York, 1989), Vol.19, Chap. 2.